CellPress

Review

# Brain Oscillations and the Importance of Waveform Shape

Scott R. Cole[1,*] and Bradley Voytek[1,2,3,4]

**Oscillations are a prevalent feature of brain recordings. They are believed to play key roles in neural communication and computation. Current analysis methods for studying neural oscillations often implicitly assume that the oscillations are sinusoidal. While these approaches have proven fruitful, we show here that there are numerous instances in which neural oscillations are nonsinusoidal. We highlight approaches to characterize nonsinusoidal features and account for them in traditional spectral analysis. Instead of being a nuisance, we discuss how these nonsinusoidal features may provide crucial and so far overlooked physiological information related to neural communication, computation, and cognition.**

## Trends

The properties of neural oscillations are commonly correlated to disease or behavior states. These measures are mostly derived using traditional spectral analysis techniques that assume a sinusoidal basis.

Electrical recordings from many brain regions, at multiple spatial scales, exhibit neural oscillations that are nonsinusoidal.

New methods have been developed to quantify the nonsinusoidal features of oscillations and account for these features when using traditional spectral analysis.

Features of oscillatory waveform shape have been related to physiological processes and behaviors.

Manipulating the features of stimulation waveforms changes the effects of rhythmic electrical stimulation.

## Neural Oscillation Characterization

Rhythms in neural activity are observed across various temporal and spatial scales and are often referred to as **oscillations** (see Glossary) [1]. Traditionally, neural oscillations have been clustered into canonical frequency bands, including delta (1–4 Hz), theta (4–8 Hz), alpha (8–12 Hz), beta (15–30 Hz), gamma (30–90 Hz), and high gamma (>50 Hz). These bands roughly correspond to frequency ranges commonly observed in human electroencephalography (EEG) studies. Although they have been observed for nearly a century, recent theories suggest that these oscillations play an active role in neural communication [2].

One prominent theory is that oscillations accomplish this function using **cross-frequency coupling (CFC)**, in which multiple neural oscillators in different frequency ranges interact with one another [3]. To characterize this coupling, the **phase** and **amplitude** properties of each oscillator are calculated using **spectral analysis**. A key feature in all spectral analysis methods is that they inherently assume that the fluctuations in brain activity over time can be characterized using a **sinusoidal** basis. That is, the underlying assumption is that the complexities of oscillatory brain activity are best captured by sinusoidal oscillators. A sinusoid (or sine wave) is a smoothly varying rhythmic signal governed by a mathematical equation. However, as we will discuss below, neural oscillations are commonly **nonsinusoidal**. Instead of being a nuisance, we argue that these nonsinusoidal features may contain crucial physiological information about the neural systems and dynamics that generate them.

We address here the inconsistency between standard neural analysis approaches and the observed nonsinusoidal shapes of oscillatory waveforms. We begin by reviewing a diverse set of examples of nonsinusoidal oscillations across species. Interestingly, studies published before the modern proliferation of advanced computation have focused more on raw, unfiltered data, by necessity. By contrast, recent studies tend to focus on heavily processed data and lack attention to the oscillatory waveform shapes. We discuss methodological approaches for

[1]Neurosciences Graduate Program, University of California, San Diego, La Jolla, CA, USA
[2]Department of Cognitive Science, University of California, San Diego, La Jolla, CA, USA
[3]Institute for Neural Computation, University of California, San Diego, La Jolla, CA, USA
[4]Kavli Institute for Brain and Mind, University of California, San Diego, La Jolla, CA, USA

*Correspondence: scott.cole0@gmail.com (S.R. Cole).

characterizing nonsinusoidal features of neural oscillations, as well as adaptations to traditional spectral analysis to account for nonsinusoidal waveforms. Thus, combining waveform shape analysis with a modern understanding of the physiological generators of neural oscillations can provide an entirely new framework for understanding the physiological basis of neural computation and cognition.

## Nonsinusoidal Waveforms Are Stereotyped

One strong indication that the waveform shape of neural oscillations contains physiological information is that features of these waveforms are stereotyped across recordings. This consistency indicates that the waveform shape reflects something specific about the physiology of the recorded brain region. We review here several examples of this phenomenon.

In human electrophysiology, oscillations with stereotyped nonsinusoidal shapes include the sensorimotor 'mu rhythm', motor cortical beta oscillation, and cortical 'slow oscillations'. The mu rhythm oscillates at an alpha frequency (around 10 Hz) and was named because its waveform shape resembles the Greek character μ (Figure 1A). It is characterized by the fact that one extremum (e.g., its peak) is consistently **sharper** than the other (e.g., its trough); it is also described as an **arch**, comb, or wicket shape [4–10].

In addition to the sensorimotor mu rhythm, we have recently highlighted that motor cortical beta oscillations also have striking nonsinusoidal features [11]. These beta oscillations manifest a **sawtooth** shape in that their voltage either rapidly rises before more slowly falling off, or vice versa (Figure 1B).

In contrast to these faster rhythms, 'slow oscillations' are low-frequency rhythms (<1 Hz) that dominate across the cerebral cortex during anesthesia and natural sleep [12–14]. Slow oscillations are distinguished by alternating periods of depolarization (up-states, positive half-wave in surface EEG) and hyperpolarization (down-states, negative half-wave in surface EEG) [12]. The negative half-waves are consistently sharper than the positive half-waves, again resulting in a stereotyped arch-like shape [15–19]. Because the waveform shapes of these oscillations are relatively conserved across brain regions, individuals, and even species, we reason that these oscillation features likely contain information about the oscillatory generators. Because of the assumptions of standard sinusoid-based spectral analyses, these potentially crucial nonsinusoidal features will be lost or overlooked.

Animal models also give us an opportunity to invasively record nonsinusoidal oscillations that are often not feasible to record in humans. Hippocampal theta oscillations, for example, are among the best-studied rhythms in the local field potential (LFP); they have a stereotyped sawtooth shape (Figure 1C) [20–26]. Similarly, respiratory rhythms in the olfactory bulb are also sawtooth-like in shape [26,27]. While slow oscillations are arch-shaped when recorded with macroelectrodes, those recorded in the LFP have complex and diverse shapes, with sharp transitions between the up- and down-states (Figure 1D) [12,26,28,29]. These invasive recordings present a unique opportunity to extract information from waveform shape because of their closer proximity to the signal source.

If the waveform shape of an oscillation reflects physiology that is truly evolutionarily conserved, we expect to see similar waveform features in analogous oscillations across species. One example of such conservation is the stereotyped sawtooth waveform of the hippocampal theta rhythm that is observed in rabbit, mouse, and rat [20,30,31]. In addition, arch-shaped alpha-frequency oscillations are observed in rat somatosensory cortex, and these have been hypothesized to be analogous to the previously mentioned mu rhythms in EEG [32,33]. Furthermore, slow oscillations are also arch-shaped in surface EEG in the anesthetized cat [12], to give only

## Glossary

**Amplitude:** the magnitude of an oscillation in a signal, measured in volts.
**Arch:** a periodic waveform in which one extremum is consistently sharper than the opposite.
**Cross-frequency coupling (CFC):** a biophysical interaction between two oscillators with different fundamental frequencies.
**Multiplex:** multiple streams of information encoded in a single signal.
**Nonsinusoidal:** an oscillatory waveform shape that deviates from a sine wave.
**Oscillation:** a periodic component of a time series, such that the phase at one timepoint can be predicted by the phase at a past timepoint. In electrical recordings, the voltage fluctuates between two extremes, with some variability in frequency and amplitude.
**Phase:** a point in a periodic cycle, such as the peak, trough, or zero-crossing.
**Phase–amplitude coupling (PAC):** a subtype of CFC defined by a statistical correlation between the phase of one oscillation and the amplitude of a second oscillation. Oscillations can be from the same recording ('within-channel') or from separate simultaneously recorded channels ('cross-channel')
**Sawtooth:** a periodic waveform that fluctuates between two extrema with a fast rise (or decay) and a slow, linear decay (or rise).
**Sharpness:** a description of the shape of oscillatory extrema. Extrema are relatively sharp if the rate of voltage change around the extrema is relatively high.
**Sinusoid:** the imaginary component of the trajectory at a constant angular frequency along a circle in the complex plane. The sinusoid is a smoothly varying periodic signal that has special mathematical properties, allowing it to be used as the basis for the Fourier transform. A sinusoid is defined by its frequency, amplitude, and phase.
**Spectral analysis:** a family of techniques used to quantify the phase and amplitude of a neural oscillation by focusing on a small frequency range of interest.
**Spike-wave discharges:** a stereotyped waveform that is commonly observed in epileptic

three examples. Concerning slow oscillations, Amzica and Steriade presaged in 1998 that 'Fourier spectra are not able to discriminate between periodic phenomena and waves with a given shape', noting that analyses 'should take into consideration the actual aspect of waves and, if possible, their relationship with the state of the cellular aggregates of the corticothalamic network' [12]. We extend this sentiment here to all neural oscillations.

In addition to the variety of empirical reports, theoretical estimates of field activity acquired through computational modeling are also notably nonsinusoidal. A common method for simulating gamma oscillations, for example, is the biophysically inspired pyramidal-interneuron gamma (PING) cortical model. In a morphologically realistic simulation of the LFP, gamma oscillations show a sawtooth-like waveform shape; while the decay phase was very short, the

tissue. The waveform consists of a brief, sharp spike and a slower wave.
**Transient:** a high-magnitude deflection in a time series that lasts a short period of time.

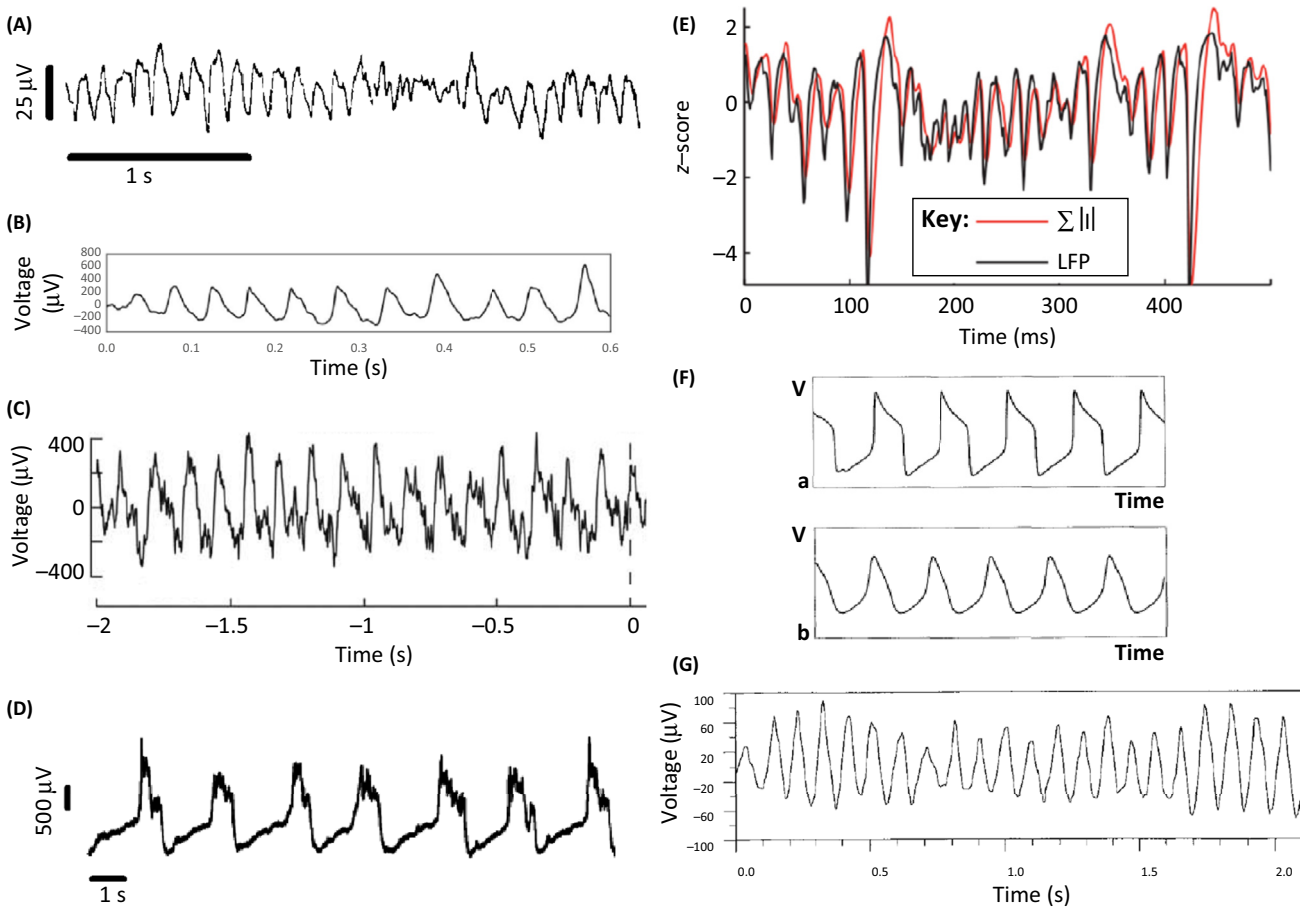


Trends in Cognitive Sciences

Figure 1. Oscillatory Waveforms Are Nonsinusoidal in Many Neural Recordings and Simulations. (A) The mu rhythm, a motor cortical oscillation with power at 10 Hz, is characterized by its sharp extrema which produce an arch shape. Reproduced, with permission, from [8]. (B) Beta oscillations in the human primary motor cortex (ECoG) have sharp and sawtooth-like features. Produced by the authors. (C) Theta oscillations in the rodent hippocampus have a sawtooth-like waveform in which oscillatory rises are steeper than decays. Reproduced, with permission, from [23]. (D) Slow oscillations in the neocortex have complex waveforms that contain aspects of arches, sawtooths, and rectangular waves. Reproduced, with permission, from [28]. (E) Gamma oscillations produced by the pyramidal–interneuron gamma (PING) mechanism. Field potentials were generated both in a population of morphologically realistic neurons (black) and by using a weighted sum of synaptic currents (red). In both cases the waveforms had an asymmetric shape: a sharp voltage drop followed by an exponential-shaped voltage rise. Reproduced, with permission, from [72]. (F) The waveform shape of a conductance-based Morris–Lecar oscillator model changes with the lambda parameter (a: lambda = 0.02, b: lambda = 0.33), though they are never truly sinusoidal. Note that the top example is strikingly similar to the temporal dynamics of slow oscillations recorded in the parietal cortex of rats (see panel D). Reproduced, with permission, from [35]. (G) A type of alpha oscillations in the rat gustatory cortex (LFP) have a complicated arch waveform that disappears at taste delivery (dotted line). Reproduced, with permission, from [55]. Abbreviations: ECoG, electrocorticography; LFP, local field potential.

voltage rise had an exponentially decaying trajectory, analogous to synaptic currents (Figure 1E). By comparison, a slightly different implementation of the PING model yielded gamma oscillations with an arch shape [34]. The different oscillatory shapes generated by different PING models are driven by differences in the defined biophysical parameters, hinting at a link between biophysics and waveform shape.

Other computational models of neural oscillations are more abstract and do not directly simulate the synaptic currents that largely underlie the LFP. Even so, the waveform generated by a Morris–Lecar model [35] (Figure 1F, top) has a strikingly similar waveform to the slow oscillations shown in Figure 1D. By changing the parameters of the model oscillators, researchers can fit simulated waveforms to those recorded in the LFP. In theory, this technique of altering biophysical parameters in LFP simulations to fit waveform shape can be inverted to try to infer biophysical parameters from the LFP. This could prove to be an enticing extension to the common analytic toolkit used to study oscillations, moving beyond standard spectral analyses to more physiologically informed approaches.

## Methods for Characterizing Nonsinusoidal Oscillations

Given the numerous examples of stereotyped oscillatory waveforms described above, metrics have been developed to quantify the features of the waveform shape, although they are underutilized. We recently quantified the sharpness of peaks and troughs by calculating the short-term voltage change around each extrema in the raw trace [11]. The ratio between peak and trough sharpness was shown to differentiate neural activity between neurological treatment conditions in Parkinson's disease (PD). In addition to the symmetry of oscillatory peaks and troughs, other studies have quantified the symmetry between the rise and decay phases to determine how rapidly the voltage rises compares to its decay time. The ratio between the rise time and decay time has been used to quantify the sawtooth nature of the hippocampal theta rhythm, where the rise phase is consistently shorter than the decay phase [21,22]. Similarly, a 'slope ratio' has been used to compare the steepness of the rise period to that of the adjacent decay period [36]. While promising, these metrics do not capture the full space of possible waveform features, and more approaches will need to be developed to further characterize oscillatory waveforms. Links between nonsinusoidal waveform shape and physiology will be more accurate by measuring multiple waveform features.

In addition to quantifying features of the waveform shape, methods have been developed to account for nonsinusoidal waveforms when performing traditional spectral analysis. Nonsinusoidal oscillations have been shown to generate unintuitive phase and amplitude estimates [22,37–39]. The amplitude of high-frequency oscillations is spuriously increased when filtering sharp **transients** [39]. To correct for this, a classifier was developed to differentiate between sharp events with and without high-frequency oscillations [39]. Because the hippocampal theta waveform has such a striking sawtooth shape, some researchers studying the phase of this oscillation have developed alternative waveform-based phase estimates that interpolate between empirically identified timepoints, including extrema and zero-crossings [21–23,40]. Using this approach, it was shown that decoding the spatial position of a rat is improved by referencing spiking to this alternate phase estimate as compared to traditional sinusoidal phase estimates [21].

Because both phase and amplitude estimates can be unintuitive for nonsinusoidal oscillations, waveform shape is an important consideration in **phase–amplitude coupling (PAC)** analysis, which quantifies the correlation between the phase of one oscillator and the amplitude of a higher-frequency oscillator. Box 1 contains extended discussion of how nonsinusoidal oscillations can lead to misleading PAC results. Similar concerns regarding phase–phase coupling are discussed in Box 2. Past studies have provided various recommendations for assessing

### Box 1. Nonsinusoidal Oscillations Influence PAC Estimates

PAC is estimated by quantifying the relationship between the phase of a low-frequency oscillation and the amplitude of a higher-frequency oscillation or broadband. Numerous reports have used both real and simulated data to show that nonsinusoidal oscillations with stereotyped sharp transients increase PAC estimates [11,36,38,41,42,44,45,87]. The presence of nonsinusoidal waveforms and sharp transients, rather than the ubiquity of PAC across the cortex, might reasonably explain why significant PAC exists in a majority of cortical electrode recordings [85]. However, a recent review concluded less than 15% of papers reporting PAC discuss the possibility that it is biased by nonsinusoidal oscillations [43].

Coupling between two oscillators can be clearly observed in some raw traces, including in the hippocampus (e.g., [70,88]) and subthalamic nucleus (e.g., [89]). In these cases, the power spectra contain peaks in both frequency bands of interest, and coupling is specific to these frequencies. This stands in contrast to reports of coupling between broadband power (50–200 Hz) and a broad range of low-frequency oscillations [90–93]. While this can be interpreted as a form a oscillatory **multiplexing** [94], wherein numerous low-frequency bands can couple to local spiking/high gamma, such broadband coupling can also arise from nonsinusoidal waveform features [11,44–46]. Rather than ubiquitous coupling across multiple overlapping neural oscillators, these reports of broad low-frequency phase to high-gamma coupling might be better explained by changes in the synchrony of synaptic bursts, which is known to alter low-frequency waveform shape [73].

The accuracy of phase estimates increases with the relative power of the oscillation [43]. However, only around half of articles accounted for power changes in their PAC analyses [43]. This control is crucial when comparing PAC metrics between conditions in which the low-frequency band power changes significantly. For example, several studies have reported both a desynchronization of beta oscillations at movement onset as well as a decrease in beta–high-gamma PAC estimates [91,93,95,96]. This reduced beta–high-gamma PAC estimate with movement has been interpreted as evidence that the beta rhythm actively gates motor function [93]. However, such an estimated PAC change may invoke alternative physiological interpretations if some of the motor cortical beta oscillations are sharp, as is observed in similar ECoG recordings [11].

The risk of cross-channel CFC arising from nonsinusoidal features may be lower than within-channel CFC because the phase and amplitude estimates are obtained from separate signals. However, apparent cross-channel CFC can also arise if the populations recorded by the two electrodes are driven by common input [43]. Therefore, analyses of cross-channel CFC should be controlled by within-channel analyses, such as within-channel PAC, as well as by cross-channel phase coherence.

whether PAC is true or spurious [38,41–46]. We suggest here that the spurious/non-spurious dichotomy may not be useful because 'spurious' implies uninformative. By contrast, we argue that the apparent PAC that arises from nonsinusoidal features is still a valid measure of signal properties, although the biophysical interpretation may differ depending on the waveform

### Box 2. Nonsinusoidal Oscillations Influence Phase–Phase Coupling (PPC) Estimates

Within-channel cross-frequency PPC has been reported as a potential mechanism for information selection and routing [97]. When the frequency of the two coupled phases are integer multiples of one another, this is referred to as *n:m* coupling. For example, 3:1 phase synchrony occurs if a 60 Hz oscillation has three cycles in each cycle of a 20 Hz oscillation, such that the peaks of these two oscillators consistently align.

PPC has been reported most prominently across the cortex [97] and in the hippocampus [21]. Cortical PPC exists simultaneously across many frequency bands within a channel [97,98]. However, similarly to ubiquitous PAC, it is possible that nonsinusoidal features extracted using sinusoidal basis functions can give the appearance of multiplexed PPC. Instead, the relevant features of the signal may more parsimoniously be explained by characterizing the oscillatory waveform. This was recently demonstrated in that hippocampal theta–gamma PPC does not statistically differ from chance because the sawtooth-shaped theta oscillation is necessarily phase-coupled to its harmonics [99].

Some reports of PPC have included counter-arguments to the possibility that the coupling is generated by nonsinusoidal oscillations. For example, a difference between the cortical topography of alpha and beta power has been cited to support the existence of true coupling [100]. However, this topographical difference is also consistent with topographical changes in the waveform shape of alpha oscillations, as seen in the central mu rhythm, which contains increased harmonic power compared to the occipital alpha oscillation. Others have argued that positive amplitude correlations are required if nonsinusoidal oscillations underlie PPC [97]. Ultimately, waveform shape should be analyzed to clarify the temporal dynamics underlying reported PPC.

properties that give rise to the observed PAC. That is, statistically significant PAC may not indicate two interacting oscillators at different frequencies, but instead may reflect one regular nonsinusoidal oscillator.

PAC methods have been recently adapted to account for nonsinusoidal oscillations. Because nonsinusoidal oscillations produce a nonuniform distribution of instantaneous phase, PAC estimates may be biased, and a correcting factor based on phase nonuniformity was suggested [37]. This nonuniform phase distribution also confounds analyses of phase-locked spiking, which can be appropriately addressed using surrogate statistics [47]. As for amplitude estimates, the previously mentioned classifier that detects true high-frequency oscillations was applied to assess PAC changes while avoiding the confounding effects of sharp transients [48]. Ultimately, measuring the waveform shape of oscillations would clarify the implications of PAC estimates.

While nonsinusoidal oscillations are not parsimoniously captured in the components of the Fourier transform, alternative decomposition methods have been applied to study neural oscillations [49–52]. In contrast to techniques such as the Fourier transform, the matching pursuit algorithm decomposes the signal using transient broadband functions in addition to narrowband functions, making it suitable for capturing physiologically informative sharp waveform features [50]. Another approach, empirical mode decomposition (EMD), decomposes a signal into rhythmic components based on local extrema rather than on sinusoidal components. One study showed that EMD improved the frequency resolution of coupling in both simulated data and mouse hippocampal recordings [52]. EMD was also applied to analyze amplitude–amplitude coupling in an attempt to account for the fact that such coupling is positively biased by nonsinusoidal and nonstationary oscillations [53]. Thus, decomposition methods that do not assume a sinusoidal basis may be more appropriate for analyzing the spectral properties of oscillations with a nonsinusoidal waveform shape.

While such approaches require multiple oscillatory cycles to yield useful metrics, studying the temporal dynamics of single oscillatory cycles can also reveal crucial physiological information, as previously suggested [25,38]. The fast (30–60 Hz) arch-shaped oscillations produced in response to cortical injury in the rabbit are relevant here [54]. At the start of injury, monophasic spikes appear in isolation, but gradually become broader and more frequent, generating an arch-shaped oscillation, followed by a quasi-sinusoidal oscillation. From a nonsinusoidal perspective, each period of the oscillation has its own interesting temporal dynamics. Therefore, analysis of each period as an individual event may be more appropriate than analyzing the series of events as one oscillatory process.

## Distinguishing between Different Oscillatory Processes by Waveform Shape

The aforementioned methods for quantifying the features of oscillatory waveforms can be used to distinguish between oscillatory phenomena that appear at similar spatial locations, and at the same frequency, but have different physiological origins. Because distinct neural processes can coexist in the same frequency band, applying a narrow bandpass filter may make multiple distinct oscillatory processes indistinguishable from one another. For example, in the rat gustatory cortex there are three alpha-frequency rhythms that appear to be distinct because they occur at a specific time during a sensory experience and can be distinguished by their waveform shape in addition to their center frequency and amplitude [55].

Similarly, two of the earliest identified signals in human EEG were the visual cortical alpha oscillation and the aforementioned sensorimotor mu rhythm. Because of their sometimes overlapping spatial topographies and frequencies (8–12 Hz), the two oscillations can be misidentified and confused with one another [56]. However, an important difference between these

two rhythms is their waveform shape. As mentioned above, the mu rhythm has an arch-like waveform while, By contrast, the occipital alpha oscillation has a more symmetric waveform that even appears characteristically triangular in some raw traces (e.g., [57]) (Figure 1G). These differences in shape likely reflect differences in the properties of these two oscillatory generators. The sharp transient of the mu rhythm is hypothesized to reflect a current source in the primary somatosensory hand area [10]. The occipital alpha oscillation may manifest as a smoother waveform because the underlying current source is less temporally synchronous. This hypothesized difference in physiology is analogous to previous hypotheses regarding the differences in the shapes of slow oscillations [12].

In addition to slow oscillations, 1–5 Hz sawtooth-shaped waves also occur in human EEG and are particularly associated with rapid eye movement (REM) sleep [58–60]. Noting the shape of this rhythm has helped to associate it with distinct behaviors and mechanisms that would not have been possible if it was simply filtered and identified as a 'delta oscillation'. In addition, sleep spindles are characterized as bursts of 8–14 Hz oscillations that are observed during sleep, together with slow oscillations and sawtooth waves. Sleep spindle subtypes can be distinguished by their shape [61].

## Oscillation Waveform Shape Relates to Physiology

Robust differences in the waveform shapes of the oscillations mentioned above can be assumed to represent differences in the properties of their underlying generators. For example, the sharp transients that occur in **spike-wave discharges**, as well as in an alpha rhythm in the gustatory cortex, correspond to synchronous local spiking [62–65]. By contrast, the smooth 'wave' component of the spike-wave discharge coincided with a slow depolarization of layer 5/6 neurons [66]. The 'spike' portion of this waveform was preceded by a layer-specific firing pattern, coincided with fast depolarization, and was followed by fast hyperpolarization of these layer 5/6 neurons. Given the known variability of the generators for spike-wave discharge shapes [64], quantifying differences in waveform shape may explain some differences in the type or stage of epilepsy.

Waveform shape differences are also observed within a region. The longer duration of slow oscillation up-states in the infragranular layers (below pyramidal cell bodies) compared to supragranular layers (above pyramidal cell bodies) contains information on how the slow oscillation is generated across layers [29]. By analyzing multielectrode recordings throughout the hippocampus, the hilar region has consistently been observed to have the most sinusoidal oscillations (see 'hil' in Figure 2A) [67–69]. These results suggest that the electrical properties of these oscillations are nonuniform across the region, even if the whole region contains power at the same frequency.

In addition to differences across cortical layers, waveform shape may also contain information about the neurotransmitters that are present. Again in the hippocampus, the addition of atropine, which blocks acetylcholine receptors, resulted in more irregular theta oscillations, as characterized by broader distributions in cycle length and trough amplitude (Figure 2B) [70]. By contrast, urethane anesthesia makes the theta oscillation more symmetric [67]. Addition of kainate to hippocampal slices induced gamma oscillations that were more sawtooth-shaped than spontaneously generated gamma oscillations [71]. The near-instantaneous voltage drop followed by an exponentially decaying voltage rise observed in the kainate-induced gamma oscillations is strikingly similar to the gamma oscillations produced in a previously mentioned PING model [72]. In summary, these experiments suggest that the shape of the LFP may index the influence of neurotransmitters on neurophysiology. However, because reports analyzing waveform shape are sparse, it is difficult to generalize these results.

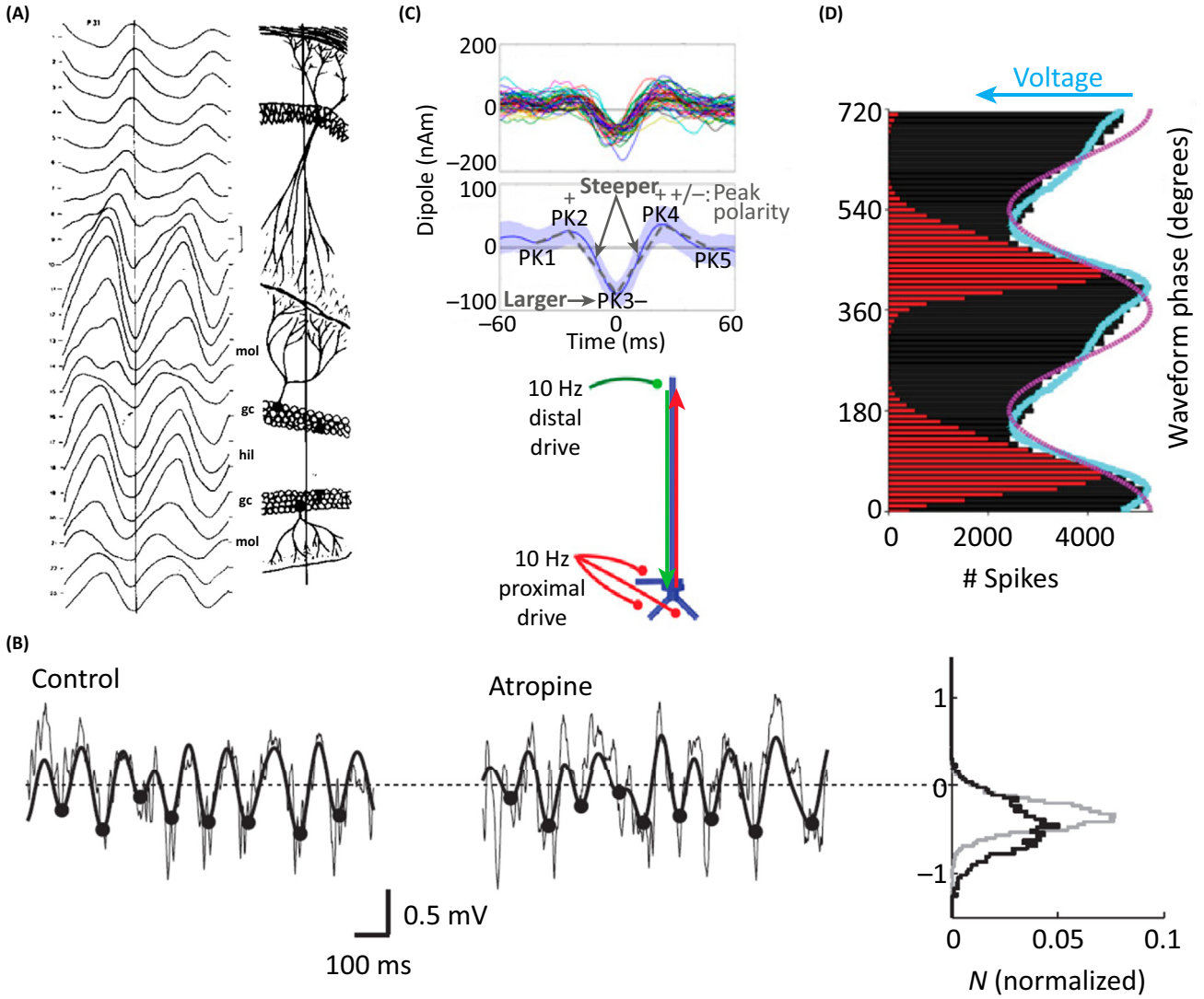


Trends in Cognitive Sciences

Figure 2. Features of Nonsinusoidal Waveforms Relate to Physiology. (A) The shapes of hippocampal theta oscillations change as a function of recording depth. Reproduced, with permission, from [67] (gc, granule cell layer; hil, hilus; mol, molecular layer). (B) Theta oscillations recorded in mouse hippocampus during exploration without (left) or with (center) the addition of atropine. The voltage at each trough is indicated with a dot, and the distributions of voltages are represented in histograms (right). Addition of atropine blocks muscarinic acetylcholine receptors and causes the trough voltage to be more variable (broader, black histogram). Reproduced, with permission, from [70]. (C) Transient beta oscillations in human somatosensory cortex recorded by magnetoencephalography (MEG). (Top) Examples of raw beta oscillations aligned to the largest trough. (Center) The average waveform (shading, SD) has a sharp, steep center transient. (Bottom) This waveform shape was reproduced in a model by synchronous excitatory synaptic drive both distal and proximal to the soma. Reproduced, with permission, from [73]. (D) The temporal dynamics of extracellular theta oscillations relate to those of firing rates. The firing histogram (#, number of spikes) color indicates if the spike occurred in the rise of a theta oscillation (red) or the decay (black). The blue line indicates the median voltage of the theta oscillation in each phase bin. The purple line is a sinusoid of comparable frequency. Note that the nonsinusoidal voltage trace is more highly correlated to the population firing rate compared to the sinusoid. Reproduced, with permission, from [21].

Attempts to explain distinct waveform shapes can inspire models of their physiological generation. A recent study did exactly this for the transient beta oscillations recorded by magnetoencephalography (MEG) in primary somatosensory cortex (S1) and right inferior frontal cortex (IFC) (Figure 2C) [73]. The S1 beta waveform is shaped such that the central trough is sharper and more negative than the adjacent troughs, consequently making its flanks relatively steep. It was proposed that the transient oscillations could be generated by nearly synchronous excitatory

synaptic burst inputs into the proximal and distal dendrites of pyramidal cells. However, the relative sizes of the peaks and troughs differed between S1 and IFC; follow-up studies incorporating more physiological and architectural features may be able to explain this difference.

For some oscillations, waveform shape may be a surrogate for the population firing rate throughout a period. This relates trivially to slow oscillations in which one extremum is associated with greater local firing whereas the opposite phase is associated with lower firing. In addition, asymmetric peaks in a slow oscillation period are indicative of strong spiking in that cycle [74], and the sawtooth shape of hippocampal theta oscillations tracks firing rate better than a comparable sinusoid (Figure 2D) [21]. However, the amount of firing rate variance explained by the oscillation waveform in general is unclear, and likely differs by the identity of the oscillator being studied. In a model of cortical gamma oscillations, the population firing rate was a candidate proxy for the biophysically computed LFP ($R^2 > 0.5$) [72]. However, waveform shape may not reflect solely neural processes because glial membrane potentials are synchronized to slow oscillations and have similar shapes [12,13].

As suggested earlier, the shape of an oscillatory waveform can be analyzed to test whether it is consistent with a proposed model of generation. This has been used, for example, in one modeling study that generated gamma oscillations using two different mechanisms. These two oscillators manifested waveforms that differed in slope ratio (defined above), predicting different waveform shapes [36]. In another example, an oscillation generated by pulsing inhibition has been hypothesized to produce an oscillation with 'amplitude asymmetry' [75]. Amplitude asymmetry occurs when the trough voltage remains constant while the peak voltage fluctuates (or vice versa). Thus it has been proposed that pulsing inhibition is the underlying mechanism of some MEG oscillations projected to occipital, central, and parietal areas that have this property [75–78]. This model is consistent with known inhibitory feedback from the neocortex and thalamus [75], but direct empirical evidence to confirm this model is needed.

Causal evidence of the computational importance of oscillatory waveform shape comes from studies applying oscillatory neurostimulation. Modifying the shape of the stimulating waveform, while preserving amplitude and frequency, resulted in changes in the efficiency of entraining local population spiking in slices [29] and alpha oscillations in human EEG [79]. In both cases it was concluded that the steep slopes of the nonsinusoidal stimulation are key in entraining the network, reminiscent of a previous modeling result showing that nonsinusoidal oscillators synchronize faster to one another compared to more sinusoidal oscillators [35]. Relatedly, rectangular waves induce seizures more reliably than sine waves for electroconvulsive therapy [80,81], and sine wave stimulation is associated with greater memory loss and more intense seizures [82,83]. In summary, the effects of neurostimulation vary greatly with the stimulating waveform, suggesting that electrical waveforms generated by the brain may also impact on neural computation in different ways.

## Oscillatory Waveform Shape Relates to Disease and Behavior States

Two recent studies have compared the shape of neural oscillations between disease states. In anesthetized rats, the relative duration of up- and down-states were measured in parietal cortical slow oscillations [28]. There was no difference in slow oscillation frequency between rats developing epilepsy compared to control animals. However, the rats developing epilepsy had relatively longer up-states. Recently we used electrocorticography (ECoG) to analyze primary motor cortex of patients with PD who had undergone implantation of a permanent deep brain stimulator (DBS) [11]. Oscillations were most asymmetric in regards to peak and trough sharpness in recordings from untreated Parkinsonian patients compared to those same patients when their DBS was turned on (Figure 3A). Sharpening of oscillatory beta extrema may

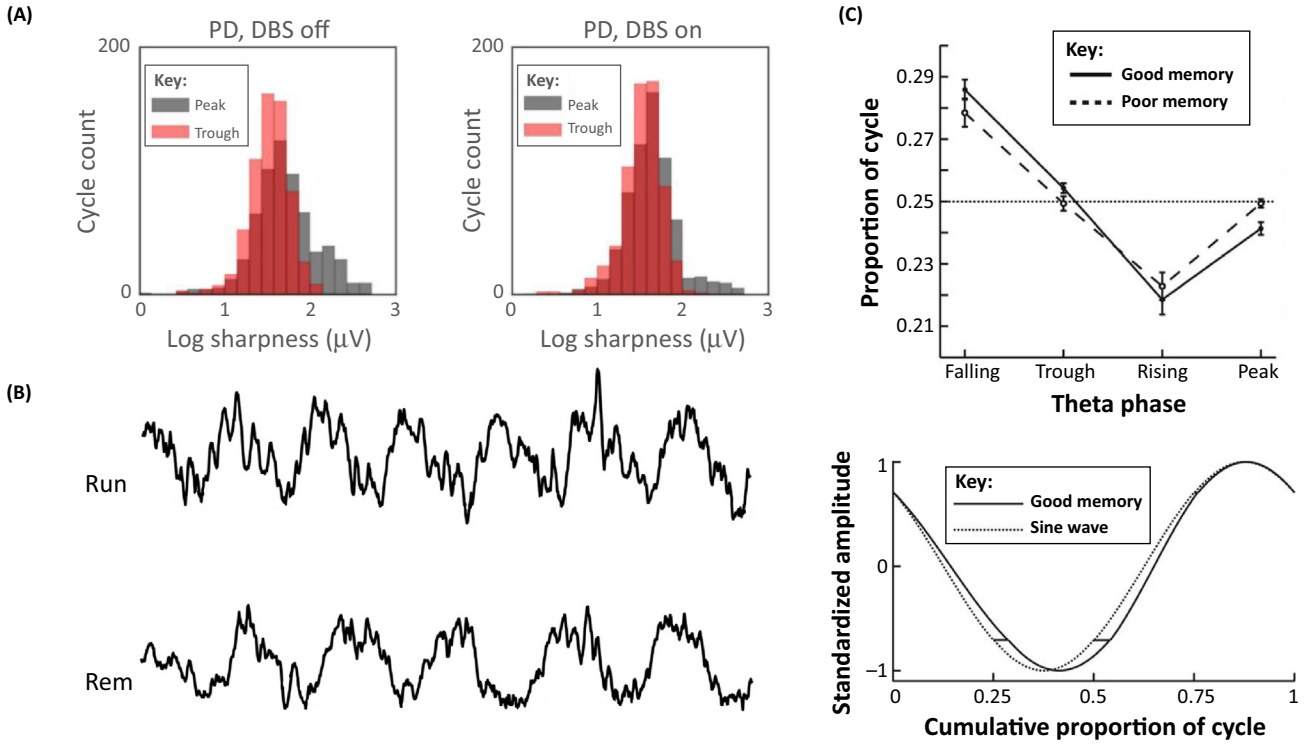


Figure 3. Features of Oscillatory Waveforms Relate to Behavior and Disease. (A) The sharpness of the peaks and troughs of motor cortical beta oscillations were measured in Parkinson's disease (PD) patients. The overlaps in peak and trough sharpness distributions are lower in PD patients with an implanted deep brain stimulator (DBS) turned off (left) compared to when it is turned on (right). In other words, the sharpness ratio between the peaks and troughs is greater in untreated PD patients, as visualized by a separation in the distributions of peak and trough sharpness. Reproduced, with permission, from [11]. (B) Hippocampal theta oscillations in rats are more asymmetric while the rat is running (RUN, top) than when the rat is sleeping (REM, bottom). During running, theta oscillations generally have a steeper rise to the peak and a more gradual decay to the trough. Reproduced, with permission, from [21]. (C) Hippocampal theta oscillation symmetry also differed in rats based on memory performance. During a successful encoding period of an object, the theta oscillation was more asymmetric in that its falling phase was extended and its rising phase was shortened. Reproduced, with permission, from [23].

reflect an increase in the synchrony of synaptic bursts [73] that is thought to be pathological in PD.

There is mounting evidence that the prominent hippocampal theta oscillation shape is altered with behavior. In particular, the aforementioned sawtooth shape of hippocampal theta has been reported to become more asymmetric (i.e., approaching the instantaneous voltage change that characterizes a pure sawtooth) when a rat is running, compared to during immobility [70], lever pressing [20], or REM sleep [21] (Figure 3B). This change in the asymmetry of hippocampal theta oscillations during running must reflect a change in the rhythmic neural computation. Future studies could identify the mechanisms associated with changes in theta asymmetry and what significance this has for running behavior. A similar analysis on theta oscillations was performed during memory-encoding periods [23]. During the encoding of objects that were subsequently remembered (compared to subsequently forgotten), the hippocampal theta oscillation of the rat was more asymmetric (Figure 3C). There was no accompanying change in theta frequency or amplitude. The authors theorized that this elongation of the theta oscillation falling slope improved memory by enhancing CA3–CA1 gamma coherence. Future studies can test this hypothesis by using electrical or optogenetic stimulation to manipulate the shape of the theta waveform in CA1.

## Concluding Remarks

We have reviewed a broad literature showing that oscillations have diverse waveform shapes. These nonsinusoidal features likely relate to physiology, making it theoretically possible to infer physiology from waveform shape. Importantly, this idea has been hinted at or directly mentioned in several earlier reports [12,23,36,38,43,49,51,84,85]; however, such reports of waveform shape have been brief and sparse in the literature of neural oscillations. While relatively novel in neuroscience, nonsinusoidal oscillations emerge in other physical phenomena with associated methods for addressing these features. For example, the chemical-processing industry applies curve-fitting algorithms to identify nonsinusoidal waveforms in control loops (e.g., [86]).

Future efforts in experimental design, analytical method development, and computational modeling should explicitly probe how differences in waveform shape relate to differences in physiology (see Outstanding Questions). For example, rhythmic stimulation experiments (electric, magnetic, optogenetic, etc.) can vary the stimulating waveform and assess behavioral or physiological differences. In addition, simultaneous recordings of field potentials and neuronal spiking will help us to quantify relationships between waveform shape, synchrony, and other spiking features. It may even be possible to move past the sinusoidal assumptions of the Fourier transform and toward more biologically informed decomposition methods, perhaps consisting of a 'dictionary' of neurophysiological basis functions (as similarly suggested in [38]). Finally, and perhaps of great immediate interest, existing experimental data containing neural oscillations can be re-analyzed to inspect waveform shape. New empirical results will in turn inspire novel analytical methods and computational models to drive new theories regarding how oscillation waveform relates to their underlying biophysical generators.

## Outstanding Questions

Can a 'dictionary' of biophysically informed oscillatory shapes be used as a more principled decomposition tool, compared to the set of sinusoidal basis functions of the Fourier transform?

What are the most biophysically informative features that can be extracted from an oscillatory waveform (e.g., rise-time to decay-time ratio). How do each of these features potentially relate to physiological processes (e.g., neural firing synchrony)?

Is it possible to predict how changes in the physical structure or network connectivity in a brain region affect the waveforms of oscillatory processes recorded in that region?

To what extent does noise corrupt information represented in the shape of oscillatory waveforms?

For what diseases can oscillatory waveform shape be a useful biomarker of pathology?

How does manipulating the oscillatory waveform shape of electrical or optogenetic stimulation differentially affect the neural circuit?

How stable are the shapes of different neural oscillations over time?

### Acknowledgments

We thank Richard Gao, Tammy Tran, and Roemer van der Meij for comments on the manuscript, and Erik Peterson, Tom Donoghue, Colin Hoy, Chris Holdgraf, Nicole Swann, and Brad Postle for invaluable discussion. S.R.C. is supported by the National Science Foundation Graduate Research Fellowship Program. B.V. is supported by the University of California, San Diego, the Qualcomm Institute, California Institute for Telecommunications and Information Technology, Strategic Research Opportunities Program, and a Sloan Research Fellowship.

### References

1. Buzsáki, G. (2006) *Rhythms of the Brain,* Oxford University Press
2. Fries, P. (2005) A mechanism for cognitive dynamics: neuronal communication through neuronal coherence. *Trends Cogn. Sci.* 9, 474–480
3. Canolty, R.T. and Knight, R.T. (2010) The functional role of cross-frequency coupling. *Trends Cogn. Sci.* 14, 506–515
4. Arroyo, S. *et al.* (1993) Functional significance of the mu rhythm of human cortex: an electrophysiologic study with subdural electrodes. *Electroencephalogr. Clin. Neurophysiol.* 87, 76–87
5. Pfurtscheller, G. *et al.* (2006) Mu rhythm (de)synchronization and EEG single-trial classification of different motor imagery tasks. *Neuroimage* 31, 153–159
6. Pfurtscheller, G. *et al.* (1997) On the existence of different types of central beta rhythms below 30 Hz. *Electroencephalogr. Clin. Neurophysiol.* 102, 316–325
7. Muthukumaraswamy, S.D. *et al.* (2004) Mu rhythm modulation during observation of an object-directed grasp. *Cogn. Brain Res.* 19, 195–201
8. Kuhlman, W.N. (1978) Functional topography of the human mu rhythm. *Electroencephalogr. Clin. Neurophysiol.* 44, 83–93
9. Salmelin, R. and Hari, R. (1994) Spatiotemporal characteristics of sensorimotor neuromagnetic rhythms related to thumb movement. *Neuroscience* 60, 537–550
10. Tiihonen, J. *et al.* (1989) Magnetic mu rhythm in man. *Neuroscience* 32, 793–800
11. Cole, S.R. *et al.* (2016) Nonsinusoidal oscillations underlie pathological phase–amplitude coupling in the motor cortex in Parkinson's disease. *bioRxiv.* Published online April 19, 2016. http://dx.doi.org/10.1101/049304
12. Amzica, F. and Steriade, M. (1998) Electrophysiological correlates of sleep delta waves 1. *Electroencephalogr. Clin. Neurophysiol.* 107, 69–83
13. Amzica, F. and Steriade, M. (2000) Neuronal and glial membrane potentials during sleep and paroxysmal oscillations in the neocortex. *J. Neurosci.* 20, 6648–6665
14. Steriade, M. *et al.* (1993) A novel slow (<1 Hz) oscillation of neocortical neurons *in vivo*: depolarizing and hyperpolarizing components. *J. Neurosci.* 13, 3252–3265
15. Massimini, M. (2002) EEG slow (~1 Hz) waves are associated with nonstationarity of thalamo-cortical sensory processing in the sleeping human. *J. Neurophysiol.* 89, 1205–1213
16. Massimini, M. (2004) The sleep slow oscillation as a traveling wave. *J. Neurosci.* 24, 6862–6870
17. Ngo, H.V.V. *et al.* (2013) Auditory closed-loop stimulation of the sleep slow oscillation enhances memory. *Neuron* 78, 545–553
18. Mölle, M. *et al.* (2002) Grouping of spindle activity during slow oscillations in human non-rapid eye movement sleep. *J. Neurosci.* 22, 10941–10947
19. Clemens, Z. *et al.* (2007) Temporal coupling of parahippocampal ripples, sleep spindles and slow oscillations in humans. *Brain* 130, 2868–2878
20. Buzsáki, G. *et al.* (1985) Depth profiles of hippocampal rhythmic slow activity ('theta rhythm') depend on behaviour. *Electroencephalogr. Clin. Neurophysiol.* 61, 77–88

21. Belluscio, M. *et al.* (2012) Cross-frequency phase–phase coupling between theta and gamma oscillations in the hippocampus. *J. Neurosci.* 32, 423–435
22. Dvorak, D. and Fenton, A.A. (2014) Toward a proper estimation of phase-amplitude coupling in neural oscillations. *J. Neurosci. Methods* 225, 42–56
23. Trimper, J.B. *et al.* (2014) Recognition memory and theta–gamma interactions in the hippocampus. *Hippocampus* 24, 341–353
24. Green, J.D. and Petsche, H. (1961) Hippocampal electrical activity II. Virtual generators. *Electroencephalogr. Clin. Neurophysiol.* 13, 847–853
25. Artemenko, D.P. (1972) Role of hippocampal neurons in theta-wave generation. *Neurophysiology* 4, 531–539
26. Lockmann, A.L.V. *et al.* (2016) A respiration-coupled rhythm in the rat hippocampus independent of theta and slow oscillations. *J. Neurosci.* 36, 5338–5352
27. Buonviso, N. *et al.* (2003) Rhythm sequence through the olfactory bulb layers during the time window of a respiratory cycle. *Eur. J. Neurosci.* 17, 1811–1819
28. Ouedraogo, D.W. *et al.* (2016) Abnormal UP/DOWN membrane potential dynamics coupled with the neocortical slow oscillation in dentate granule cells during the latent phase of temporal lobe epilepsy. *eNeuro* 3, ENEURO-0017
29. Frohlich, F. and McCormick, D.A. (2010) Endogenous electric fields may guide neocortical network activity. *Neuron* 67, 129–143
30. Buzsáki, G. *et al.* (2003) Hippocampal network patterns of activity in the mouse. *Neuroscience* 116, 201–211
31. Bland, B.H. *et al.* (1980) Automated analysis of rhythmicity of physiologically identified hippocampal formation neurons. *Exp. Brain Res.* 38, 205–219
32. Fransen, A.M. *et al.* (2016) Distinct alpha and beta band rhythms over rat somatosensory cortex with similar properties as in humans. *J. Neurophysiol* 115, 3030–3044
33. Wiest, M.C. and Nicolelis, M.A.L. (2003) Behavioral detection of tactile stimuli during 7-12 Hz cortical oscillations in awake rats. *Nat. Neurosci.* 6, 913–914
34. Lowet, E. *et al.* (2016) Quantifying neural oscillatory synchronization: a comparison between spectral coherence and phase-locking value approaches. *PLoS One* 11, e0146443
35. Somers, D. and Kopell, N. (1993) Rapid synchronization through fast threshold modulation. *Biol. Cybern.* 68, 393–407
36. Lee, S. and Jones, S.R. (2013) Distinguishing mechanisms of gamma frequency oscillations in human current source signals using a computational model of a laminar neocortical network. *Front. Hum. Neurosci.* 7, 869
37. van Driel, J. *et al.* (2015) Phase-clustering bias in phase–amplitude cross-frequency coupling and its removal. *J. Neurosci. Methods* 254, 60–72
38. Jones, S.R. (2016) When brain rhythms aren't 'rhythmic': implication for their mechanisms and meaning. *Curr. Opin. Neurobiol.* 40, 72–80
39. Amiri, M. *et al.* (2016) High frequency oscillations and spikes: separating real HFOs from false oscillations. *Clin. Neurophysiol.* 127, 187–196
40. Siapas, A.G. *et al.* (2005) Prefrontal phase locking to hippocampal theta oscillations. *Neuron* 46, 141–151
41. Kramer, M.A. *et al.* (2008) Sharp edge artifacts and spurious coupling in EEG frequency comodulation measures. *J. Neurosci. Methods* 170, 352–357
42. Ray, S. and Maunsell, J.H.R. (2011) Different origins of gamma rhythm and high-gamma activity in macaque visual cortex. *PLoS Biol.* 9, e1000610
43. Aru, J. *et al.* (2015) Untangling cross-frequency coupling in neuroscience. *Curr. Opin. Neurobiol.* 31, 51–61
44. Lozano-Soldevilla, D. *et al.* (2016) Neuronal oscillations with non-sinusoidal morphology produce spurious phase-to-amplitude coupling and directionality. *Front. Comput. Neurosci.* 10, 1–17
45. Gerber, E.M. *et al.* (2016) Non-sinusoidal activity can produce cross-frequency coupling in cortical signals in the absence of functional interaction between neural source. *PLoS One* 11, e0167351
46. Vaz, A.P. *et al.* (2016) Dual origins of measured phase-amplitude coupling reveal distinct neural mechanisms underlying episodic memory in the human cortex. *bioRxiv.* Published online October 28, 2016. http://dx.doi.org/10.1101/084194
47. Sigurdsson, T. *et al.* (2010) Impaired hippocampal–prefrontal synchrony in a genetic mouse model of schizophrenia. *Nature* 464, 763–767
48. Amiri, M. *et al.* (2016) Phase–amplitude coupling is elevated in deep sleep and in the onset zone of focal epileptic seizures. *Front. Hum. Neurosci.* 10, 1–12
49. Bullock, T.H. *et al.* (2003) Are the electroencephalograms mainly rhythmic? Assessment of periodicity in wide-band time series. *Neuroscience* 121, 233–252
50. Chandran, K.S.S. *et al.* (2016) Comparison of matching pursuit algorithm with other signal processing techniques for computation of the time-frequency power spectrum of brain signals. *J. Neurosci.* 36, 3399–3408
51. Mäkinen, V.T. *et al.* (2005) The use of stationarity and nonstationarity in the detection and analysis of neural oscillations. *Neuroimage* 28, 389–400
52. Pittman-Polletta, B. *et al.* (2014) Detecting phase–amplitude coupling with high frequency resolution using adaptive decompositions. *J. Neurosci. Methods* 226, 15–32
53. Yeh, C-H. *et al.* (2016) Spurious cross-frequency amplitude–amplitude coupling in nonstationary, nonlinear signals. *Physica A* 454, 143–150
54. Adrian, E.D. and Matthews, B.H.C. (1934) The interpretation of potential waves in the cortex. *J. Physiol.* 81, 440–471
55. Tort, A.B.L. *et al.* (2010) Cortical networks produce three distinct 7-12 Hz rhythms during single sensory responses in the awake rat. *J. Neurosci.* 30, 4315–4324
56. Pineda, J.A. (2005) The functional significance of mu rhythms: translating 'seeing' and 'hearing' into 'doing'. *Brain Res. Rev.* 50, 57–68
57. Stam, C.J. *et al.* (1999) Dynamics of the human alpha rhythm: evidence for non-linearity? *Clin. Neurophysiol.* 110, 1801–1813
58. Louis, R.P. *et al.* (2004) Design and validation of a computer-based sleep-scoring algorithm. *J. Neurosci. Methods* 133, 71–80
59. Berger, J.R. *et al.* (1962) The EEG, eye-movement and dreams of the blind. *Q. J. Exp. Psychol.* 14, 183–186
60. Pearl, P.L. *et al.* (2002) Sawtooth wave density analysis during REM sleep in normal volunteers. *Sleep Med.* 3, 255–258
61. Pavlov, a.N. *et al.* (2012) Wavelet analysis in neurodynamics. *Uspekhi Fiz. Nauk* 182, 905
62. Fabricius, M. *et al.* (2008) Association of seizures with cortical spreading depression and peri-infarct depolarisations in the acutely injured brain. *Clin. Neurophysiol.* 119, 1973–1984
63. Coenen, A.M.L. and Van Luijtelaar, E.L.J.M. (2003) Genetic animal models for absence epilepsy: a review of the WAG/Rij strain of rats. *Behav. Genet.* 33, 635–655
64. Slaght, J. *et al.* (2004) On the activity of the corticostriatal networks during spike-and-wave discharges in a genetic model of absence epilepsy. *J. Neurosci.* 24, 6816–6825
65. Fontanini, A. (2005) 7 to 12 Hz activity in rat gustatory cortex reflects disengagement from a fluid self-administration task. *J. Neurophysiol.* 93, 2832–2840
66. Polack, P-O. *et al.* (2007) Deep layer somatosensory cortical neurons initiate spike-and-wave discharges in a genetic model of absence seizures. *J. Neurosci.* 27, 6590–6599
67. Buzsáki, G. *et al.* (1986) Laminar distribution of hippocampal rhythmic slow activity (RSA) in the behaving rat: current-source density analysis, effects of urethane and atropine. *Brain Res.* 365, 125–137
68. Montgomery, S.M. *et al.* (2009) Behavior-dependent coordination of multiple theta dipoles in the hippocampus. *J. Neurosci.* 29, 1381–1394
69. Konopacki, J. *et al.* (1988) Carbachol-induced EEG 'theta' in hippocampal formation slices: evidence for a third generator of theta in CA3c area. *Brain Res.* 451, 33–42

70. Hentschke, H. *et al.* (2007) Muscarinic blockade weakens interaction of gamma with theta rhythms in mouse hippocampus. *Eur. J. Neurosci.* 26, 1642–1656

71. Pietersen, A.N.J. *et al.* (2009) Comparison between spontaneous and kainate-induced gamma oscillations in the mouse hippocampus *in vitro*. *Eur. J. Neurosci.* 29, 2145–2156

72. Mazzoni, A. *et al.* (2015) Computing the local field potential (LFP) from integrate-and-fire network models. *PLoS Comput. Biol.* 11, 1–38

73. Sherman, M.A. *et al.* (2016) Neural mechanisms of transient neocortical beta rhythms: converging evidence from humans, computational modeling, monkeys, and mice. *Proc. Natl. Acad. Sci. U. S. A.* 113, E4885–E4894

74. Lewis, L.D. *et al.* (2012) Rapid fragmentation of neuronal networks at the onset of propofol-induced unconsciousness. *Proc. Natl. Acad. Sci. U. S. A.* 109, E3377–E3386

75. Mazaheri, A. and Jensen, O. (2010) Rhythmic pulsing: linking ongoing brain activity with evoked responses. *Front. Hum. Neurosci.* 4, 177

76. Mazaheri, A. and Jensen, O. (2008) Asymmetric amplitude modulations of brain oscillations generate slow evoked responses. *J. Neurosci.* 28, 7781–7787

77. van Dijk, H. *et al.* (2010) Modulations in oscillatory activity with amplitude asymmetry can produce cognitively relevant event-related responses. *Proc. Natl. Acad. Sci. U. S. A.* 107, 900–905

78. Nikulin, V.V. *et al.* (2007) A novel mechanism for evoked responses in the human brain. *Eur. J. Neurosci.* 25, 3146–3154

79. Dowsett, J. and Herrmann, C.S. (2016) Transcranial alternating current stimulation with sawtooth waves: simultaneous stimulation and EEG recording. *Front. Hum. Neurosci.* 10, 1–10

80. Merritt, H. and Putnam, T. (1938) A new series of anticonvulsant drugs tested by experiments on animals. *Arch. Neurol. Psychiatry* 39, 1003–1015

81. Abrams, R. (2002) *Electroconvulsive Therapy,* Oxford University Press

82. Weiner, R.D. *et al.* (1986) Effects of electroconvulsive therapy upon brain electrical activity. *Ann. N. Y. Acad. Sci.* 462, 270–281

83. Weiner, R.D. *et al.* (1986) Effects of stimulus parameters on cognitive side effects. *Ann. N. Y. Acad. Sci.* 462, 315–325

84. Nikulin, V.V. *et al.* (2010) Non-zero mean and asymmetry of neuronal oscillations have different implications for evoked responses. *Clin. Neurophysiol.* 121, 186–193

85. He, B.J. *et al.* (2010) The temporal structures and functional significance of scale-free brain activity. *Neuron* 66, 353–369

86. Zakharov, A. and Jämsä-Jounela, S-L. (2014) Robust oscillation detection index and characterization of oscillating signals for valve stiction detection. *Ind. Eng. Chem. Res.* 53, 5973–5981

87. He, B.J. (2014) Scale-free brain activity: past, present, and future. *Trends Cogn. Sci.* 18, 480–487

88. Tort, A.B.L. *et al.* (2009) Theta–gamma coupling increases during the learning of item–context associations. *Proc. Natl. Acad. Sci. U. S. A.* 106, 20942–20947

89. van Wijk, B.C.M. *et al.* (2016) Subthalamic nucleus phase–amplitude coupling correlates with motor impairment in Parkinson's disease. *Clin. Neurophysiol.* 127, 2010–2019

90. Edakawa, K. *et al.* (2016) Detection of epileptic seizures using phase–amplitude coupling in intracranial electroencephalography. *Sci. Rep.* 6, 25422

91. Kondylis, E.D. *et al.* (2016) Movement-related dynamics of cortical oscillations in Parkinson's disease and essential tremor. *Brain* 139, 2211–2223

92. Swann, N.C. *et al.* (2015) Elevated synchrony in Parkinson disease detected with electroencephalography. *Ann. Neurol.* 78, 742–750

93. Miller, K.J. *et al.* (2012) Human motor cortical activity is selectively phase-entrained on underlying rhythms. *PLoS Comput. Biol.* 8, e1002655

94. Akam, T. and Kullmann, D.M. (2014) Oscillatory multiplexing of population codes for selective communication in the mammalian brain. *Nat. Rev. Neurosci.* 15, 111–122

95. Yanagisawa, T. *et al.* (2012) Regulation of motor representation by phase-amplitude coupling in the sensorimotor cortex. *J. Neurosci.* 32, 15467–15475

96. Qasim, S.E. *et al.* (2016) Electrocorticography reveals beta desynchronization in the basal ganglia–cortical loop during rest tremor in Parkinson's disease. *Neurobiol. Dis.* 86, 177–186

97. Palva, J.M. *et al.* (2005) Phase synchrony among neuronal oscillations in the human cortex. *J. Neurosci.* 25, 3962–3972

98. Isler, J.R. *et al.* (2008) Cross-frequency phase coupling of brain rhythms during the orienting response. *Brain Res.* 1232, 163–172

99. Scheffer-Teixeira, R. and Tort, A.B. (2016) Lack of evidence for cross-frequency phase–phase coupling between theta and gamma oscillations in the hippocampus. *bioRxiv*. Published online March 28, 2016. http://dx.doi.org/10.1101/045963

100. Nikulin, V.V. and Brismar, T. (2006) Phase synchronization between alpha and beta oscillations in the human electroencephalogram. *Neuroscience* 137, 647–657